HHS Public Access

Author manuscript

Am J Geriatr Psychiatry. Author manuscript; available in PMC 2024 January 05.

Published in final edited form as:

Am J Geriatr Psychiatry. 2023 February ; 31(2): 112–123. doi:10.1016/j.jagp.2022.09.011.

In pre-clinical AD small vessel disease is associated with altered hippocampal connectivity and atrophy

Minjie Wu, PhD[1,*], **Noah Schweitzer**[2], **Bistra E. Iordanova, PhD**[2], **Edythe Halligan-Eddy**[1], **Dana L. Tudorascu, PhD**[1,3], **Chester A. Mathis, PhD**[4], **Brian J. Lopresti, MS**[4], **M. Ilyas Kamboh, PhD**[5], **Ann D. Cohen, PhD**[1], **Beth E. Snitz, PhD**[6], **William E. Klunk, MD, PhD**[1], **Howard J. Aizenstein, MD, PhD**[1,2]

[1]Department of Psychiatry, University of Pittsburgh, Pittsburgh, PA

[2]Department of Bioengineering, University of Pittsburgh, Pittsburgh, PA

[3]Departments of Medicine and Biostatistics, University of Pittsburgh, Pittsburgh, PA

[4]Department of Radiology, University of Pittsburgh, Pittsburgh, PA

[5]Department of Human Genetics, University of Pittsburgh, Pittsburgh, PA

[6]Department of Neurology, University of Pittsburgh, Pittsburgh, PA

Abstract

Objective—Small Vessel Disease (SVD) is known to be associated with higher AD risk, but its relationship to amyloidosis in the progression of AD is unclear. In this cross-sectional study of cognitively normal older adults, we explored the interactive effects of SVD and amyloid-beta (Aβ) pathology on hippocampal functional connectivity during an associative encoding task and on hippocampal volume.

Methods—This study included sixty-one cognitively normal older adults (age range: 65-93 years, age mean ± standard deviation: 75.8 ± 6.4, 41 (67.2%) female). PiB PET, T2-weighted FLAIR, T1-weighted and face-name fMRI images were acquired on each participant to evaluate brain Aβ, white matter hyperintensities (WMH+/− status), gray matter density and hippocampal functional connectivity.

[*]Corresponding Author: Minjie Wu, Ph.D., Assistant Professor, Department of Psychiatry, University of Pittsburgh, miw75@pitt.edu, Phone: 412-246-4562.

Author Contributions

MW designed the study, analyzed the fMRI and structural MR data, interpreted the results and wrote the manuscript with helpful discussions, feedback and revision comments from all co-authors (NS, BI, EHE, DT, CM, BL, MK, AC, BS, WK, HJ). Specifically, NS helped write the manuscript, analyzed the data, and performed the statistical analyses and data interpretation. BI helped result interpretation and provided critical revision comments. EHE oversaw and performed data collections for the study. DT oversaw and provided critical comments on the statistical analyses. CM, BL, and AC assisted with the PiB PET component of this manuscript. MK determined the genotype (APOE forms) of the participants. BS supervised the neurocognitive data collection and analyses. WK and HJ supervised and designed the study, interpreted the findings, reviewed and revised this manuscript.

Competing interests

The authors declare no competing interests in relation to the work described.

Supplementary material

Supplementary material is available at *the American Journal of Geriatric Psychiatry* online.

Results—We found that, in WMH(+) older adults greater Aβ burden was associated with greater hippocampal local connectivity (i.e., hippocampal-parahippocampal connectivity) and lower gray matter density in medial temporal lobe (MTL), whereas in WMH(−) older adults greater Aβ burden was associated with greater hippocampal distal connectivity (i.e., hippocampal-prefrontal connectivity) and no changes in MTL gray matter density. Moreover, greater hippocampal local connectivity was associated with MTL atrophy.

Conclusion—These observations support a hippocampal excitotoxicity model linking SVD to neurodegeneration in pre-clinical AD. This may explain how SVD may accelerate the progression from Aβ positivity to neurodegeneration, and subsequent AD.

Keywords

Alzheimer's disease; cerebral small vessel disease; amyloid-beta; functional connectivity; atrophy

Introduction

Cerebral small vessel disease (SVD) refers to injury to small arteries, arterioles, veins, venules, and capillaries in the brain. White matter lesions (WMLs), identified as hyperintensities (WMH) on T2-weighted FLAIR MR brain images, are an important radiologic marker of SVD. SVD is very common in both non-demented elderly and late-onset Alzheimer's disease (AD) patients. Amyloid-beta (Aβ) plaques in the brain are one of the key pathological hallmarks of AD and the accumulation of Aβ starts approximately 10 to 20 years prior to the onset of clinical dementia(1–3). A mixed pathology of AD and SVD represents the most common cause of dementia in the elderly population(4). The presence of SVD has been shown to modify the clinical course of AD. Co-existing white matter lesions are associated with poorer cognitive performance, greater likelihood or earlier presence of clinical dementia and more severe clinical symptoms in AD patients(5–8). In non-demented or cognitively normal elderly adults, co-existing SVD and Aβ pathologies are associated with greater medial temporal lobe (MTL) atrophy(9) and a higher rate of cognitive decline(10). However, it remains unclear whether and how SVD may interact with Aβ pathology to affect the memory network, and modify the course of disease progression at the pre-clinical stage of AD. Therefore, the current study investigated whether the presence of SVD (measured as significant WMH burden) altered the associations between brain Aβ and hippocampal functional connectivity during associative encoding, and the associations between brain Aβ and gray matter density in the MTL in cognitively normal older adults. One potential pathway linking SVD to AD, is through hippocampal excitotoxicity. Previous animal studies have demonstrated excitotoxicity mechanisms relating hippocampal hyperactivity to neurodegeneration in AD(11–13). An excessive release of glutamate neurotransmitter can lead to a dysregulation of Ca2+ homeostasis and subsequent excitotoxicity. Thus, we hypothesized that the presence of SVD will be associated with greater hippocampal local functional connectivity and MTL gray matter atrophy in individuals with pre-clinical AD.

Materials and Methods

Participants

This study included sixty-one cognitively normal older adults (age range: 65-93 years, age mean ± standard deviation: 75.8 ± 6.4, 41 (67.2%) female). Inclusion criteria and exclusion criteria were previously described in detail(14). In brief, inclusion criteria were age ≥ 65 years, education ≥ 12 years, and fluency in English. Exclusion criteria were diagnosis of MCI or dementia, history of a major psychiatric or neurological condition, conditions affecting cognition or cognitive test performance, and MR-contraindications. To ensure cognitive normality, a comprehensive neuropsychological testing battery was conducted on all participants in multiple cognitive domains including memory, visuospatial construction, language, and attention and executive functions(15). This study was approved by the Human Use Subcommittee of the Radioactive Drug Research Committees and the Institutional Review Board of the University of Pittsburgh.

Image Acquisition and Processing

PiB PET imaging—[^{11}C]PiB (Pittsburgh Compound-B) was synthesized by a simplified radiosynthetic method described in (16). Fifteen mCi of [^{11}C]PiB with high specific activity [~2.1 Ci/μmol at end of synthesis (EOS)] was injected intravenously over 20 seconds. Beginning 50 minutes after injection, a 20-min PiB PET scanning was conducted on a Siemens/CTI ECAT HR+ scanner (Siemens Medical Solutions, Knoxville, TN) in 3D imaging mode: 4 x 300 second frames, 63 axial slices, slice thickness = 2.4mm, field of view (FOV) = 15.2cm, intrinsic in-plane resolution = 4.1 mm full-width at half-maximum (FWHM) at FOV center.

MRI acquisition—All MR scanning was performed on a 3T Siemens Trio scanner with 12-channel head coil at the University of Pittsburgh Magnetic Resonance Research Center. T1-weighted structural images were acquired axially using a magnetization-prepared rapid gradient echo sequence (T1w MPRAGE): TR = 2300 ms, TE = 3.4 ms, flip angle (FA) = 9°, FOV = 240 × 256 mm^2, matrix = 240 x 256, slice thickness/gap = 1/0 mm, and 160 slices. T2-weighted fluid-attenuated inversion recovery images were acquired axially (T2w FLAIR): TR = 9160 ms, TE = 90 ms, TI = 2500 ms, FA = 150°, FOV = 256×212 mm^2, matrix = 256×212. slice thickness/gap = 3/0 mm, and 48 slices. Whole-brain fMRI data were acquired axially using gradient-echo echo-planar imaging sequence (EPI): TR = 2 s, TE = 32 ms, FA = 90°, FOV = 256 × 256 mm^2, matrix = 128 × 128, slice thickness/gap = 4/0 mm (voxel size = 2 x 2 x 4 mm^3), and 28 slices.

Task fMRI data were collected while participants were performing a face-name associative encoding task. In this task, participants are presented with face-name association pairs, are asked to respond to each face-name association by pressing a button to designate whether they think the face and name fit each other, and are instructed to try to remember the association for a later recognition test(17). The task is a mixed block/event-related design task, with alternating blocks of novel face-name associations, familiar face-name pairs, and fixation. Each run contains four 48-second blocks, and each block presents 8 faces for 5 seconds each with 1 second of intermittent fixation. Between each block is a 25-second

fixation period. With fixations, each run was 267 seconds. A recognition test is carried out at the end of the scanning session, in which each face is presented with two names, and participants are asked to indicate which name was paired with the face during the fMRI task. Of the 61 participants in this study, 46 participants completed three runs, 11 completed two runs, and 4 completed one run of the face-name task.

PET data processing—Inter-frame motion of the [^{11}C]PiB acquisition frames was corrected using the automated image registration (AIR) algorithm(18). A summed PET image was generated over the 50-70-minute post-injection interval, co-registered with and resliced into the AC-PC (the anterior and posterior cerebral commissure) aligned MPRAGE MR image using AIR (PET-MR).

A set of volumes of interests (VOIs) were hand-drawn on the AC-PC aligned T1w image, including frontal cortex (FRC; ventral and dorsal), anterior cingulate gyrus (ACG: subgenual and pregenual), anteroventral striatum (AVS), precuneus/posterior cingulate cortex (PRC; ventral, middle and dorsal thirds), parietal cortex (PAR), lateral temporal cortex (LTC), and cerebellum (CER) (19). Regional radioactivity concentrations were calculated and converted into units of standardized uptake value (SUV) using these hand-drawn VOIs, the injected dose of [^{11}C]PIB and the subject's body mass. The unitless SUV outcome is normalized to non-specific uptake (from CER), yielding a SUV ratio (SUVR) measure(20). Regional SUVR outcomes were partial volume corrected using a previously validated method (20, 21). A global PiB retention index reflecting cerebral Aβ load is computed from the SUVR values from the six most relevant VOIs (ACG, FRC, LTC, PAR, PRC, and AVS). Participants were classified as Aβ positive or negative [Aβ(+) or Aβ(−)] by using a sparse k-means cluster analysis(22).

MR data processing

Gray matter density: Voxel based morphometry (VBM) with Diffeomorphic Anatomic Registration Through Exponentiated Lie Algebra (DARTEL) (SPM12) was performed on T1w MPRAGE and T2w FLAIR images(23). Warped GM probability maps were modulated by the Jacobian determinants of the deformations to correct for local expansion or contraction, which were then smoothed with an isotropic 8 mm-FWHM Gaussian kernel(24).

White Matter Hyperintensities: WMH on T2 FLAIR images were segmented using an automated method, developed based on our previous work(25). Given the observation that there were very few lesions in the cerebellum in our sample, the mean and standard deviation of cerebellar WM were used to Z-transform the T2w FLAIR image (Z-T2w FLAIR). Voxels with z score >= 2 and within the cerebral WM mask were identified as WMH. The participants were divided into two groups, i.e., the High WMH [WMH(+)] group and the Low WMH [WMH(−)] group, using a median split of WMH volumes (median WMH volume = 3.77 cubic centimeter-cc).

Functional Connectivity: Functional images were preprocessed in SPM12 for slice timing correction, motion correction, image co-registration and normalization, and spatially

smoothed (an isotropic 8mm-FWHM Gaussian filter). Generalized psychophysiological interaction (gPPI) analysis (26) was performed to estimate hippocampal functional connectivity. Two seed regions, left and right hippocampus, from the automated anatomical labeling (AAL) atlas were used (27). Principal time series (i.e., the eigenvariate) was generated for each seed region, left and right hippocampus, using singular value decomposition (SVD) from hippocampal fMRI data during the face-name task. Principal time series of the seed region (left or right hippocampus), task conditions (experimental condition: novel face-name pairs and control condition: familiar repeated face-name pairs), interaction variables (seed times series × task condition), as well as motion parameters were included in the design matrix. Functional connectivity map (left or right hippocampus) during associative encoding (i.e., novel face-name pairs versus familiar face-name pairs) was computed for each participant.

Second-level analyses

Multiple linear regression analyses were performed with hippocampal functional connectivity as the outcome variable, WMH status [WMH(+) versus WMH(−)], Aβ load, as well as the interaction of WMH status and Aβ load as independent variable while controlling for age and sex. In brain areas without significant interaction effect, analyses of variance (ANOVAs) were performed to test main effects of WMH and Aβ load, controlling for age and sex. In these analyses, Aβ burden was treated as a continuous variable (global PiB SUVR) as this project focused on pre-clinical stage of AD. To control for multiple comparisons, joint height and extent thresholds were determined via Monte Carlo simulations (10,000 iterations) with an a priori medial temporal and frontal lobe mask (AlphaSim, AFNI) for a corrected $p < 0.05$. The medial temporal and frontal lobe mask was created from the AAL atlas(27)(a total volume of 540.43 cc).

Similarly multiple linear regression analyses were performed to test the interaction between WMH and Aβ load, main effects of WMH and Aβ load on gray matter density in the medial temporal lobe. The medial temporal lobe was created from the AAL atlas (a total volume of 202.27 cc).

For post-hoc analyses, region of interest (ROI) masks were created from hippocampal and prefrontal regions that showed significant WMH x Aβ interactions. Functional connectivity and regional gray matter density values were extracted from these ROIs. To dissect the direction of the interaction and the magnitude of the effect size, partial correlations were performed in SPSS to examine the relationships between hippocampal functional connectivity, gray matter density and Aβ load stratified by WMH status, controlling for age and sex. Further, Pearson correlations were performed in SPSS to explore the relationship between hippocampal connectivity and gray matter density.

Results

Participant characteristics

Table 1 and Supplementary Table 1 summarize demographic, clinical characteristics and neurocognitive scores, stratified by WHM status. The WMH(+) and WMH(−) groups did

not significantly differ on sex, education, race, APOE status, global PiB SUVR, Aβ(+)%, or Mini–Mental State Examination (MMSE) scores. The WMH(+) group (mean age = 78.1 years) was significantly older than the WMH(−) group (mean age = 73.5 years) at the time of MR scan ($p = 0.005$). By design, the WMH(+) group (mean WMH volume = 12.1 cc) had significantly more WMH burden than the WMH(−) group (mean WMH volume = 2.6 cc) ($p<0.001$).

Neurocognitive outcomes

ANOVAs were conducted examining the main effects of WMH [WMH(+) vs. WMH(−)], Aβ [Aβ(+) vs Aβ(−)], and their interactions on the 16 different neurocognitive measures in visual spatial construction, language, attention, executive, and memory domains (See Supplementary Table 1). The only effects that withstood Bonferroni multiple comparison correction for the 48 different tests (.05/48 = 0.001) was the main effect of Aβ and the interaction of Aβ and WMH on the Trail Making B task. Detailed uncorrected statistical results were shown in Supplementary Table 1, which may suggest a possible effect but would need to be tested *a priori*.

Functional connectivity

Table 2 summarizes the main and interaction effects of WMH and Aβ load on right and left hippocampal functional connectivity during associative encoding, controlling for age and sex (corrected $p < 0.05$). In order to show the trend effect from left hippocampal connectivity (details as discussed below), Figure 1 left panel, reflecting the interaction effects of WMH x Aβ load, is presented here with a less stringent threshold (uncorrected $p < 0.01$). The scatterplots (Figure 1 right panel) were created with ROIs that survived multiple comparison (Table 2, corrected $p < 0.05$).

Right hippocampal functional connectivity.—Figure 1A and Figure 1B demonstrate significant WMH x Aβ interactions with local connectivity between right hippocampus and right parahippocampus and hippocampus (R PH/HP) regions (Figure 1A), and with distal connectivity between right hippocampus and bilateral ACC (Figure 1B).

To better understand the interaction between WMH and Aβ load, we extracted voxelwise and mean connectivity from regions with significant interaction (R PH/HP and ACC in Fig. 1 left panels). The extracted functional connectivity (beta weights) was voxelwise plotted against Aβ load in the scatterplots (small dots: voxelwise beta estimate, bold dots: mean beta estimate across ROIs). Specifically, in WMH(+) participants Aβ load was positively correlated with local connectivity between right hippocampus and R PH/HP (partial correlation coefficient $pr(27) = 0.45$, $p = 0.01$, 95% confidence interval CI [0.13 0.68]), controlling for age and sex. Conversely, in WMH(−) participants Aβ load was negatively correlated with local connectivity between right hippocampus and R PH/HP ($pr(26) = -0.70$, $p < 0.001$, 95% CI [−0.87 −0.24]), and positively correlated with distal connectivity between right hippocampus and anterior cingulate cortex ($pr(26) = 0.54$, $p = 0.003$, 95% CI [0.29 0.79]). Right hippocampal connectivity with R PH/HP or with ACC did not significantly correlate with the face/name recognition accuracy (p's > 0.15), or with cognitive measures (p's>0.09).

Left hippocampal functional connectivity.—Figure 1C (uncorrected $p < 0.01$) showed significant WMH x Aβ load interaction on functional connectivity between left hippocampus and left hippocampus and parahippocampus (L HP/PH). This area encompassed the very tail of L HP, which was at different spatial location of hippocampus compared to the findings from right hippocampus. Figure 1C also presents clusters that showed a trend toward a significant WMH x Aβ load interaction (uncorrected $p < 0.01$) at a similar brain location where the right hippocampal connectivity showed WMH x Aβ interactions. Specifically, WMH(+) participants showed Aβ-related increase in local connectivity between left hippocampus and left parahippocampus/hippocampus (uncorrected p<0.01, cluster size 41, peak $t = 3.72$) while WMH(−) participants showed Aβ-related increase in distal connectivity between left hippocampus and ACC (uncorrected $p < 0.01$, two clusters: 54x8 mm3 and 41x8 mm3, peak t = −2.97). However, these interactions were similar for left hippocampus and right hippocampus, but the effects were weaker for left hippocampus, and did not survive multiple comparisons.

There were significant main effects of WMH on functional connectivity between right hippocampus and right supplementary area (SMA), and between left hippocampus and left precentral/middle frontal gyrus (MFG). There was significant main effect of Aβ load on connectivity between left hippocampus and right MFG/inferior frontal gyrus (IFG).

Gray matter density

Table 3 summarizes the main and interaction effects of WMH and Aβ load on gray matter density in medial temporal lobe, controlling for age and sex. There were significant interaction effects between WMH and Aβ load on gray matter density in right anterior parahippocampus/hippocampus (R Ant PH/HP) and in left anterior parahippocampus/hippocampus (L Ant PH/HP) (Figure 2, corrected $p < 0.05$). Specifically, Aβ load was negatively correlated with mean gray matter density in bilateral Ant PH/HP in WMH(+) participants (R Ant PH/HP: $pr(27) = -0.45$, $p = 0.02$, 95% CI [−0.74 0.09], and L Ant PH/HP: $pr(27) = -0.413$, $p = 0.03$, 95% CI [−0.69 0.15]), but not in WMH(−) participant (p's > 0.18). Mean gray matter density in Ant PH/HP was not significantly associated with the face-name recognition accuracy, but was positively associated with Boston naming scores (R Ant PH/HP: $r(58) = 0.39$, $p = 0.002$, 95% CI [0.24 0.55] and L Ant PH/HP: $r(58) = 0.34$, $p = 0.008$, 95% CI [0.16 0.53]) and with block design scores (R Ant PH/HP: $r(58) = 0.25$, $p = 0.05$, 95% CI [−0.01 0.34] and L Ant PH/HP: $r(58) = 0.18$, $p = 0.16$).

There was no significant main effect of WMH on gray matter density in the MTL. Greater Aβ load was associated with lower gray matter density in bilateral hippocampus.

Association between functional connectivity and gray matter density

Greater local functional connectivity between right hippocampus and right PH/PH was associated with lower gray matter density in anterior parahippocampus and hippocampus (right Ant PH/HP $r(59) = -0.29$, $p = 0.02$ and left Ant PH/HP: $r(59) = -0.28$, $p = 0.03$). Greater distal functional connectivity between right hippocampus and ACC was marginally associated with greater gray matter density in left Ant PH/HP ($r(59) = -0.24$, $p = 0.06$) but not in right Ant PH/HP ($r(59) = 0.20$, $p = 0.13$).

Discussion

This study investigated the impact of WMH burden [WMH(+) and WMH(−)] on Aβ-related differences in hippocampal functional connectivity and MTL gray matter density. There are three main findings. First, in participants with significant WMH burden [WMH(+)], greater Aβ load was accompanied by greater hippocampal local connectivity (between hippocampus and parahippocampus/hippocampus), whereas in participants with minimum WMH burden [WMH(−)], greater Aβ load was associated with greater distal hippocampal-prefrontal connectivity (between hippocampus and ACC). Second, WMH(+) participants showed Aβ-related differences in gray matter density in anterior hippocampus and parahippocampus, but WMH(−) participants did not. We interpret the lower gray matter density in those with Aβ burden as hippocampal atrophy. Third, across the entire sample greater hippocampal local connectivity was associated with greater gray matter atrophy in anterior parahippocampus and hippocampus.

The classic brain “disconnection” model that structural disconnection can lead to functional disruption may explain our findings. Different patterns of hippocampal connectivity may relate to white matter disruption in WMH(+) participants, compared to WMH(−) participants. The presence of WMHs in the brain has been shown to disrupt normal appearing white matter (NAWM) close to the boundaries of WM lesions through a local penumbra effect(28), and also disrupt white matter tracts traversing WM lesions through a Wallerian-type degeneration pattern leading to an extended injury along the tracts into NAWM(29, 30). Previous studies have demonstrated the association between WMH burden and the microstructural integrity of the fornix and cingulum bundle, two major white matter tracts connecting bilateral hippocampi to subcortical and cortical brain regions. Fractional anisotropy of the fornix was negatively associated with WMH volume(31, 32). The cingulum bundle with crossing WM lesions exhibited reduced radial diffusivity compared to tracts that did not cross lesions(29). Further, hippocampal atrophy has been shown to be related to the disruption of the cingulum bundle (33). In response to increasing Aβ load, WMH(−) participants showed greater hippocampal-prefrontal connectivity, suggesting greater engagement of prefrontal regions during associative encoding. With a disconnected white matter tract network, particularly microstructural disruption in the fornix and cingulum bundle, WMH(+) participants may not be able to efficiently recruit prefrontal regions, and instead they recruit nearby resources such as hippocampus and parahippocampus, leading to a more localized pattern of activity as observed in the current study. In the disconnection model, hyperconnectivity has been conceptualized as a nonlinear process between situational/transient demands and functional information processing capacity (which relates to resource availability and neurological disruption)(34). Applying this conceptual model, local hippocampal-MTL hyperconnectivity in WMH(+) and Aβ(+) older adults with normal cognition may reflect a functional response between challenging associative memory encoding (situational/transient demands) and limitation of information processing capacity, due to white matter disruption and Aβ accumulation.

Besides greater local hippocampal-MTL functional connectivity, individuals with significant WMH and Aβ burden also showed lower gray matter density in MTL. In line with our findings, previous studies using ADNI data have shown that lower cerebrospinal fluid

Aβ1-42 and higher temporal WMH volumes were associated with smaller entorhinal cortex volume among individuals with amnestic mild cognitive impairment (MCI)(35), and that WMH were associated with a greater atrophy rate of hippocampus in nondemented older adults and in individuals with mild cognitive impairment (MCI)(36). Further, our study found that greater local hippocampal-MTL hyperconnectivity was associated with greater MTL atrophy. Excitotoxity mechanisms relating regional hyperactivity to neurodegenerative diseases have been implicated in animal studies(12). It is possible that local hippocampal-MTL hyperactivity/hyperconnectivity may signify subsequent neural excitotoxicity, and eventually lead to atrophy in the medial temporal lobe. Perhaps through this excitotoxity pathway (local hippocampal hyperconnectivity -> excitotoxity -> atrophy), SVD exacerbates the progression from Aβ positivity to neurodegeneration at the pre-clinical stage of AD.

There are current debates whether the SVD and AD pathologies additively or interactively affect neurodegeneration and cognitive decline(37). Some studies show additive or independent effects of SVD and Aβ deposition(9, 10, 38), while others show interactive effects(39, 40) on cognitive decline and medial temporal atrophy. Our findings support that there is a synergistic effect of SVD and Aβ pathologies on hippocampal functional connectivity and MTL atrophy. These finding may explain individual differences in disease trajectories. Characterizing differences in responses for AD-related pathologies, as in the current study, can help guide the development of personalized prevention and treatment strategies.

However, several important limitations of this study should be considered. The cross-sectional design of the current study is unable to establish the temporal relationship between the SVD and AD pathologies and neurodegeneration. Additional longitudinal studies are required to support the proposed order of hippocampal-MTL hyperconnectivity and MTL atrophy from SVD and AD pathologies. This study has a relatively modest sample size (N = 61). Moreover, 15 of 60 participants did not complete the entire three runs of the face-name associative encoding task, and only partial data (2 or 1 run of data) were also included in the analyses. This study enrolled cognitively normal older adults with the age of 65 years and above. It is possible that survival bias may underestimate the effects of SVD or Aβ pathologies on neurodegeneration.

When dichotomized by the mean WMH, the WMH+ group is significantly older than the WMH- group (mean age difference = 4.6 years). We statistically controlled for age in our analyses, however WMH is not independent as age is the greatest risk factor. Future studies using different components of brain age (gray matter atrophy versus white matter hyperintensities) can help disentangle the relationship between Aβ load and brain connectivity.

In this paper, we investigated the interactive effect of WMH burden and Aβ load on hippocampal functional connectivity during an associative memory fMRI task in cognitively normal older adults. We found in individuals with significant burden of WMH, Aβ load is associated with local hippocampal hyperconnectivity and medial temporal lobe atrophy. These findings support an excitotoxicity model linking SVD to an accelerated progression to neurodegeneration at the pre-clinical stage of AD. Future studies will use MR spectroscopy

(MRS) to probe the excitatory/inhibitory balance (i.e., Glutamate/GABA) in hippocampus and to further underpin related molecular pathways.

Supplementary Material

Refer to Web version on PubMed Central for supplementary material.

Funding

This work was supported by National Institute of Aging, National Institutes of Health (NIH), R01 AG067018 to MW, R01 AG063525 to HJA and ADC, RF1 AG025516 to WEK and HJA, R01 NS116450-01 to BI, and R01 AG064877, R01 AG030653 and R01 AG041718 to MIK. The content is solely the responsibility of the authors and does not necessarily represent the official views of the NIH.

Abbreviations:

AD	Alzheimer’s disease
AIR	automated image registration
Aβ	beta-Amyloid-beta
SVD	cerebral small vessel disease
EPI	echo-planar imaging
TE	echo time
FOV	field of view
fMRI	functional magnetic resonance imaging
gPPI	generalized psychophysiological interactions
MPRAGE	magnetization-prepared rapid gradient echo sequence
MTL	medial temporal lobe
MCI	mild cognitive impairment
MMSE	Mini–Mental State Examination
MNI	Montreal Neurological Institute
PiB	Pittsburgh Compound-B
TR	repetition time
SUVR	standardized uptake value ratio
T1w	T1-weighted
WML	white matter lesion
WMH	white matter hyperintensities

References

1. Perrin RJ, Fagan AM,Holtzman DM: Multimodal techniques for diagnosis and prognosis of Alzheimer's disease. Nature 2009; 461:916–922 [PubMed: 19829371]
2. Jack CR Jr., Knopman DS, Jagust WJ, et al. : Hypothetical model of dynamic biomarkers of the Alzheimer's pathological cascade. Lancet Neurol 2010; 9:119–128 [PubMed: 20083042]
3. Sperling RA, Aisen PS, Beckett LA, et al. : Toward defining the preclinical stages of Alzheimer's disease: recommendations from the National Institute on Aging-Alzheimer's Association workgroups on diagnostic guidelines for Alzheimer's disease. Alzheimers Dement 2011; 7:280–292 [PubMed: 21514248]
4. Toledo JB, Arnold SE, Raible K, et al. : Contribution of cerebrovascular disease in autopsy confirmed neurodegenerative disease cases in the National Alzheimer's Coordinating Centre. Brain 2013; 136:2697–2706 [PubMed: 23842566]
5. Snowdon DA, Greiner LH, Mortimer JA, et al. : Brain infarction and the clinical expression of Alzheimer disease. The Nun Study. JAMA 1997; 277:813–817 [PubMed: 9052711]
6. Heyman A, Fillenbaum GG, Welsh-Bohmer KA, et al. : Cerebral infarcts in patients with autopsy-proven Alzheimer's disease: CERAD, part XVIII. Consortium to Establish a Registry for Alzheimer's Disease. Neurology 1998; 51:159–162 [PubMed: 9674796]
7. Schneider JA, Wilson RS, Bienias JL, et al. : Cerebral infarctions and the likelihood of dementia from Alzheimer disease pathology. Neurology 2004; 62:1148–1155 [PubMed: 15079015]
8. Esiri MM, Nagy Z, Smith MZ, et al. : Cerebrovascular disease and threshold for dementia in the early stages of Alzheimer's disease. Lancet 1999; 354:919–920 [PubMed: 10489957]
9. Bos I, Verhey FR, Ramakers I, et al. : Cerebrovascular and amyloid pathology in predementia stages: the relationship with neurodegeneration and cognitive decline. Alzheimers Res Ther 2017; 9:101 [PubMed: 29284531]
10. Vemuri P, Lesnick TG, Przybelski SA, et al. : Vascular and amyloid pathologies are independent predictors of cognitive decline in normal elderly. Brain 2015; 138:761–771 [PubMed: 25595145]
11. Lerdkrai C, Asavapanumas N, Brawek B, et al. : Intracellular Ca(2+) stores control in vivo neuronal hyperactivity in a mouse model of Alzheimer's disease. Proc Natl Acad Sci U S A 2018; 115:E1279–E1288 [PubMed: 29358403]
12. Dong XX, Wang Y,Qin ZH: Molecular mechanisms of excitotoxicity and their relevance to pathogenesis of neurodegenerative diseases. Acta Pharmacol Sin 2009; 30:379–387 [PubMed: 19343058]
13. Zott B, Simon MM, Hong W, et al. : A vicious cycle of β amyloid–dependent neuronal hyperactivation. Science 2019; 365:559–565 [PubMed: 31395777]
14. Wu M, Thurston RC, Tudorascu DL, et al. : Amyloid deposition is associated with different patterns of hippocampal connectivity in men versus women. Neurobiol Aging 2019; 76:141–150 [PubMed: 30711677]
15. Edelman K, Tudorascu D, Agudelo C, et al. : Amyloid-Beta Deposition is Associated with Increased Medial Temporal Lobe Activation during Memory Encoding in the Cognitively Normal Elderly. Am J Geriatr Psychiatry 2017; 25:551–560 [PubMed: 28161156]
16. Wilson AA, Garcia A, Jin L, et al. : Radiotracer synthesis from [(11)C]-iodomethane: a remarkably simple captive solvent method. Nucl Med Biol 2000; 27:529–532 [PubMed: 11056365]
17. Sperling R, Chua E, Cocchiarella A, et al. : Putting names to faces: successful encoding of associative memories activates the anterior hippocampal formation. Neuroimage 2003; 20:1400–1410 [PubMed: 14568509]
18. Woods RP, Mazziotta JC,Cherry SR: MRI-PET registration with automated algorithm. J Comput Assist Tomogr 1993; 17:536–546 [PubMed: 8331222]
19. Cohen AD, Price JC, Weissfeld LA, et al. : Basal cerebral metabolism may modulate the cognitive effects of Abeta in mild cognitive impairment: an example of brain reserve. J Neurosci 2009; 29:14770–14778 [PubMed: 19940172]
20. Lopresti BJ, Klunk WE, Mathis CA, et al. : Simplified quantification of Pittsburgh Compound B amyloid imaging PET studies: a comparative analysis. J Nucl Med 2005; 46:1959–1972 [PubMed: 16330558]

21. Meltzer CC, Cantwell MN, Greer PJ, et al. : Does cerebral blood flow decline in healthy aging? A PET study with partial-volume correction. J Nucl Med 2000; 41:1842–1848 [PubMed: 11079492]
22. Cohen AD, Mowrey W, Weissfeld LA, et al. : Classification of amyloid-positivity in controls: comparison of visual read and quantitative approaches. Neuroimage 2013; 71:207–215 [PubMed: 23353602]
23. Ashburner J: A fast diffeomorphic image registration algorithm. Neuroimage 2007; 38:95–113 [PubMed: 17761438]
24. Good CD, Ashburner J,Frackowiak RS: Computational neuroanatomy: new perspectives for neuroradiology. Rev Neurol (Paris) 2001; 157:797–806 [PubMed: 11677400]
25. Wu M, Rosano C, Butters M, et al. : A fully automated method for quantifying and localizing white matter hyperintensities on MR images. Psychiatry Res 2006; 148:133–142 [PubMed: 17097277]
26. Friston KJ, Buechel C, Fink GR, et al. : Psychophysiological and modulatory interactions in neuroimaging. Neuroimage 1997; 6:218–229 [PubMed: 9344826]
27. Tzourio-Mazoyer N, Landeau B, Papathanassiou D, et al. : Automated anatomical labeling of activations in SPM using a macroscopic anatomical parcellation of the MNI MRI single-subject brain. Neuroimage 2002; 15:273–289 [PubMed: 11771995]
28. Maillard P, Fletcher E, Lockhart SN, et al. : White matter hyperintensities and their penumbra lie along a continuum of injury in the aging brain. Stroke 2014; 45:1721–1726 [PubMed: 24781079]
29. Reginold W, Itorralba J, Luedke AC, et al. : Tractography at 3T MRI of Corpus Callosum Tracts Crossing White Matter Hyperintensities. AJNR Am J Neuroradiol 2016; 37:1617–1622 [PubMed: 27127001]
30. Reginold W, Sam K, Poublanc J, et al. : Impact of white matter hyperintensities on surrounding white matter tracts. Neuroradiology 2018; 60:933–944 [PubMed: 30030550]
31. He J, Wong VS, Fletcher E, et al. : The contributions of MRI-based measures of gray matter, white matter hyperintensity, and white matter integrity to late-life cognition. AJNR Am J Neuroradiol 2012; 33:1797–1803 [PubMed: 22538073]
32. Yatawara C, Lee D, Ng KP, et al. : Mechanisms Linking White Matter Lesions, Tract Integrity, and Depression in Alzheimer Disease. Am J Geriatr Psychiatry 2019; 27:948–959 [PubMed: 31109898]
33. Villain N, Desgranges B, Viader F, et al. : Relationships between hippocampal atrophy, white matter disruption, and gray matter hypometabolism in Alzheimer's disease. J Neurosci 2008; 28:6174–6181 [PubMed: 18550759]
34. Hillary FG, Roman CA, Venkatesan U, et al. : Hyperconnectivity is a fundamental response to neurological disruption. Neuropsychology 2015; 29:59–75 [PubMed: 24933491]
35. Guzman VA, Carmichael OT, Schwarz C, et al. : White matter hyperintensities and amyloid are independently associated with entorhinal cortex volume among individuals with mild cognitive impairment. Alzheimers Dement 2013; 9:S124–131 [PubMed: 23375566]
36. Fiford CM, Manning EN, Bartlett JW, et al. : White matter hyperintensities are associated with disproportionate progressive hippocampal atrophy. Hippocampus 2017; 27:249–262 [PubMed: 27933676]
37. Liu Y, Braidy N, Poljak A, et al. : Cerebral small vessel disease and the risk of Alzheimer's disease: A systematic review. Ageing Res Rev 2018; 47:41–48 [PubMed: 29898422]
38. Gordon BA, Najmi S, Hsu P, et al. : The effects of white matter hyperintensities and amyloid deposition on Alzheimer dementia. Neuroimage Clin 2015; 8:246–252 [PubMed: 26106548]
39. Ye BS, Seo SW, Kim JH, et al. : Effects of amyloid and vascular markers on cognitive decline in subcortical vascular dementia. Neurology 2015; 85:1687–1693 [PubMed: 26468407]
40. Koncz R,Sachdev PS: Are the brain's vascular and Alzheimer pathologies additive or interactive? Curr Opin Psychiatry 2018; 31:147–152 [PubMed: 29232251]

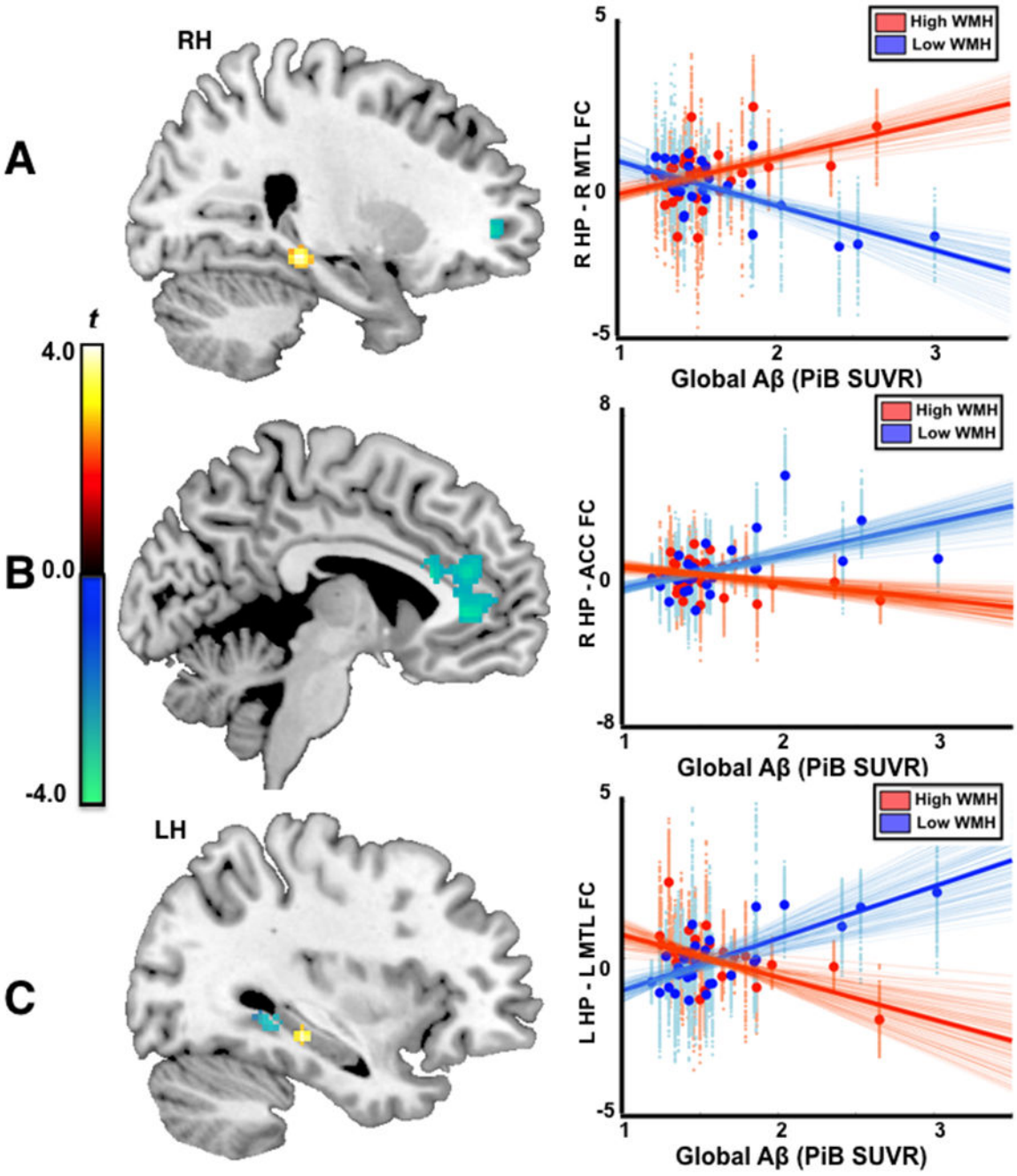

Figure 1.

There were significant interaction effects between WMH status and brain Aβ load (WMH x Aβ) on hippocampal functional connectivity. **A**. WMH x Aβ interaction on local connectivity between right hippocampus and right parahippocampus/hippocampus (R PH/HP) (left panel), and scatterplots of Aβ load and hippocampal local connectivity stratified by WMH status (Red: WMH(+)/High WMH, blue: WMH(−)/Low WMH). **B.** WMH x Aβ interaction on distal connectivity between right hippocampus and anterior cingulate cortex (ACC) (left panel), and scatterplot of Aβ load and distal hippocampal

-ACC connectivity (Red: WMH(+)/High WMH, blue: WMH(−)/Low WMH). **C.** WMH x Aβ interaction on left hippocampal connectivity (left), and scatterplots of Aβ load and connectivity between left hippocampus and L PH/PH (Red: WMH(+)/High WMH, blue: WMH(−)/Low WMH). The extracted functional connectivity (beta weights) was voxelwise plotted against Aβ load in the scatterplots (small dots: voxelwise beta estimate, bold dots: mean beta estimate across ROIs). The dark bold lines are linear fittings from mean beta estimates, with lighter lines from voxel-wise beta weights.

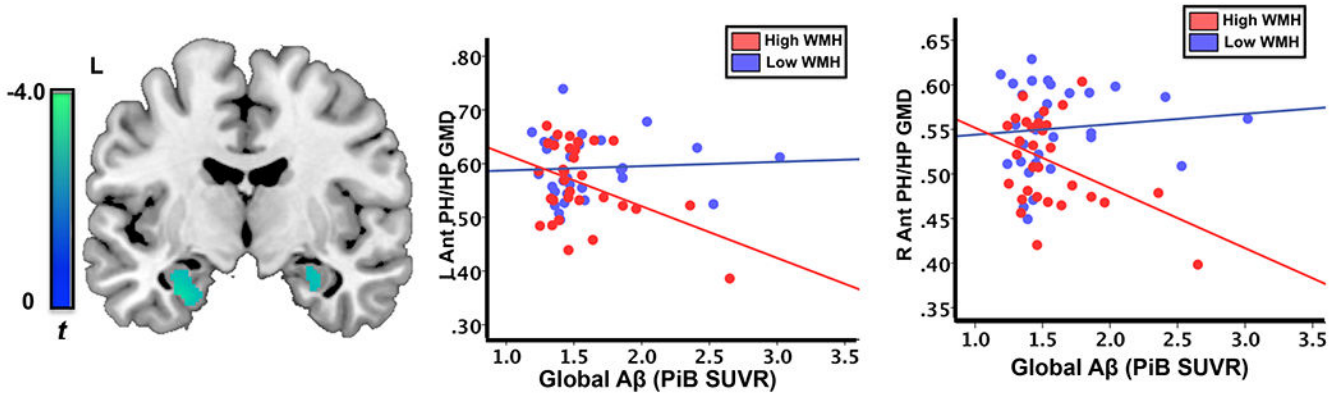

Figure 2.

There was a significant interaction between WMH status and brain Aβ load (WMH x Aβ) on gray matter density (GMD) of left anterior parahippocampus/hippocampus (L Ant PH/HP) and right anterior parahippocampus/hippocampus (R Ant PH/HP). Left: WMH x Aβ interaction on gray matter density, middle: scatterplots of Aβ load and gray matter density of L Ant PH/HP stratified by WMH status (Red: WMH(+)/High WMH, blue: WMH(−)/Low WMH), and right: scatterplots of gray matter density of R Ant PH/HP (Red: WMH(+)/High WMH, blue: WMH(−)/Low WMH).

Table 1.

Demographic variables and clinical characteristics by WMH status (N = 61[*]).

Characteristic	Group; mean (SD) WMH(+), n=31	WMH(−), n=30	Statistical test	*p* value
Age, year[†] (age range)	78.1 (6.6) [65, 93]	73.5 (5.3) [65, 83]	$F_{1,59} = 8.60$	**0.005**
Sex, female no(%)	23 (74)	18 (60)	$\chi^1 = 1.39$	0.28[♦]
Education, year	14.2 (2.1)	15.1 (2.6)	$F_{1,59} = 1.96$	0.17
Race composition, no. (%)				0.15[♦]
White	24 (77.4)	27 (90.0)		
Black	7 (22.6)	2 (6.7)		
Asian	0 (0)	1(3.3)		
APOE genotype, no. (%)[‡]				0.90[♦]
ε2/ε3	3 (12.5)	4 (20.0)		
ε3/ε3	16 (66.7)	12 (60.0)		
ε3/ε4	4 (16.7)	4 (20.0)		
ε4/ε4	1 (4.2)	0 (0.0)		
Global PiB SUVR	1.55 (0.31)	1.61 (0.41)	$F_{1,59} = 0.41$	0.52
Aβ(+), no (%)	6 (19.4)	8 (26.7)		0.55[♦]
MMSE score[§]	28.7 (1.6)	28.8 (1.2)	$F_{1,58} = 0.25$	0.62
WMH (cc)	12.1 (10.8)	2.6(0.8)	$t_{30} = 4.88$	**<0.001**
Hypertension (%)[‡]				0.58[♦]
Positive	17 (60.7)	12 (50)		
Negative	11 (39.3)	12 (50)		
Cardiovascular Disease (%)[‡]				0.56[♦]
Positive	11 (39.3)	7 (29.2)		
Negative	17 (60.7)	17 (70.8)		
Stroke History (%)[‡]				N/A
Positive	0 (0)	0 (0)		
Negative	28 (100)	24 (100)		

[*] Unless otherwise indicated.

[†] Age range 65 – 93 years.

[‡] APOE genotyping was available on 44 out of 61 participants (20 WMH(−) and 24 WMH(+)). Medical records were available on hypertension, cardiovascular disease and stroke history on 52 out of 61 participants (24 WMH(−) and 28 WMH(+)).

[§] MMSE score (Mini–Mental State Examination) was available on 60 out 61 participants (29 WMH(−) and 31 WMH(+)).

[♦] Fisher's Exact Test

Table 2.

WMH-by-Aβ load ANOVAs of hippocampal functional connectivity during the face-name associative memory task (corrected p <0.05, controlling for age and sex).

WMH -by-Aβ ANOVAs	Brain region	Brodmann area (BA)	Peak MNI coordinates (x,y,z)	t *	Size (mm^3)
Right hippocampal functional connectivity					
Main effect of WMH (WMH(+)<WMH(−))	R SMA	BA6,24	10,−2,54	3.35	616
Main effect of Aβ	None				
WMH by Aβ interaction	**R PH/HP**		**26,−32,−10**	**4.08**	**744**
	R ACC	**BA32**	**16,50,−2**	**−3.93**	**632**
	L ACC	**BA32,24**	**−8,40,2**	**−3.62**	**816**
	L ACC	**BA 32**	**−6,40,20**	**−3.32**	**528**
	R precentral/RO	**BA6,44**	**60,0,20**	**−3.79**	**1304**
Left hippocampal functional connectivity					
Main effect of WMH (WMH(+)<WMH(−))	R Precental/MFG	BA6,9	40,6,38	4.83	3088
Main effect of Aβ	R MFG/IFG	BA46	40,42,6	3.75	816
WMH by Aβ interaction	**Tail of L HP/PH**		**−28,−38,−6**	**−6.33**	**1104**

* Degree of freedom = [1, 55]

Abbreviations: MNI-Montreal Neurologic Institute; R-right, L-left; PH-parahippocampus, HP-hippocampus, SMA-supplementary motor area, ACC-anterior cingulate cortex, mPFC-medial prefrontal cortex, IFG-inferior frontal gyrus, MFG-middle frontal gyrus. Brain region PH/PH or HP/PH represents a cluster encompassing both hippocampus and parahippocampus, with PH/PH for more parahippocampal voxels and HP/PH for more hippocampal voxels in the cluster.

Table 3.

WMH-by-Aβ load ANOVAs of gray matter density in medial temporal lobe (corrected $p < 0.05$, controlling for age and sex).

WMH -by-Aβ ANOVA	Brain region	Peak MNI coordinates (x,y,z)	t*	Size (mm^3)
Main effect of WMH	None			
Main effect of Aβ	R HP	40,−25,−9	−3.89	194
	L HP	−36,−25,−6	−4.22	168
WMH by Aβ	R Ant PH/HP	34,1,−18	−3.65	470
	L Ant PH/HP	−28,−7,−27	−3.33	489

*Degree of freedom = [1, 55]

Abbreviations: MNI-Montreal Neurologic Institute; R-right, L-left; Ant-anterior, Post-posterior, PH-parahippocampus, HP-hippocampus, AMG-amygdala, MFG-middle frontal gyrus. PH/HP represents a cluster encompassing parahippocampus and hippocampus with majority of voxels belonging to parahippocampus.